Tutorial

Constraints on Metabolic Network Analysis in Bacterial Physiology

Mohammad Zim
Department of Chemical Engineering, University of Waterloo, Waterloo, ON, Canada N2L 3G1

Christian Euler
Department of Chemical Engineering, University of Waterloo, Waterloo, ON, Canada N2L 3G1 and Waterloo Centre for Microbial Research, University of Waterloo, Waterloo, ON, Canada N2L 3G1

Matthew Scott*
Department of Applied Mathematics, University of Waterloo, Waterloo, ON, Canada N2L 3G1 and Waterloo Centre for Microbial Research, University of Waterloo, Waterloo, ON, Canada N2L 3G1

(Received 3 December 2024; published 1 April 2025)

In biology, data are conceptualized using diagrams that capture protein-protein, enzyme-substrate, and regulator-target interactions, among many others. These interaction diagrams are every bit as complicated as wiring diagrams in modern electronic circuits—in many cases, even more so. Yet, in contrast to electronic circuits, living systems must also autonomously reproduce; some part of the "wiring diagram" of life must be devoted to reproducing itself. A greatly simplifying principle in the analysis of these biological wiring diagrams is that of "balanced growth," in which network flows are balanced according to the requirements of biomass production, leading to the exponential accumulation of cells. In microbial cells, exponential growth greatly simplifies the underlying biochemical networks, because when its mathematical description is combined with kinetic descriptions of underlying enzyme-mediated reactions, macroscale constraints on physiology emerge. As is demonstrated in this tutorial, these constraints are mathematically and conceptually equivalent to Kirchhoff's circuit laws and Ohm's constitutive equation. Consequently, bacterial growth physiology can be approached with the same quantitative rigour as electrical circuit analysis. In this tutorial, this "Ohmics" approach is developed in detail, and its power in simplifying complex physiology is demonstrated through two case studies.

DOI: 10.1103/PRXLife.3.022001

I. INTRODUCTION

Biological systems involve thousands of interactions of different types, operating on a wide range of timescales. This inherent complexity has frustrated attempts to establish generalizing principles to describe and predict microbial physiology. However, though the underlying interactions are complex, many of the sensible behaviors they yield can be described by emergent rules that are relatively simple.

Indeed, much of the physiology of fast-growing cells can be explained primarily by two principles: first, that the rates at which environmental materials are assimilated into biomass must be balanced according to the composition of that biomass; and second, that these rates are constrained by the autocatalytic nature of life, which necessitates that some portion of biomass must always be committed to making more biomass. Life is required to make more life. These principles were initially developed from a few observations of fast-growing cells made in the early 20th century, and they have been elaborated on since in the field of quantitative microbial physiology.

Early measurements of bacterial accumulation demonstrated that when growth is unrestricted by nutrient availability, many bacteria will convert carbon and nitrogen to biomass at a prodigious rate. For example, in nutrient-rich conditions, with a plentiful supply of oxygen and a buffer to absorb acidic waste products, the population, $N(t)$, of *Escherichia coli* cultures will double in approximately $\tau = 20$ min. During unrestricted growth, the rate of population increase is proportional to the population size,

$$\frac{dN}{dt} \propto N(t), \tag{1}$$

and if allowed to adapt to the unrestricted nutrient environment, the bacteria will reach a constant rate of growth so that the population will increase exponentially,

$$N(t) = N_0 2^{\mu t} = N_0 e^{\lambda t}, \tag{2}$$

where $\mu = 1/\tau$ is the doubling rate (typical units: doublings-per-hour), τ is the doubling time, and $\lambda = \mu \times \ln 2$ is the *specific* growth rate (typical units: per-hour).

Despite the ease with which bacterial growth can be quantified, in the early days of quantitative microbial physiology there was not a consensus on what precisely "bacterial growth" even meant, nor indeed on what physiology

*Contact author: mscott@uwaterloo.ca

yielding such growth might entail. Monod (after Buchanan) had identified several phases of bacterial growth, including the exponential phase wherein bacteria accumulate at an exponential rate, and an inevitable subsequent phase of zero net growth rate—a so-called "stationary phase" [1]. This suggested the existence of some growth limiting factor, but it was not until 1957 that Campbell [2] had the clarity of vision to define steady-state, or *balanced* growth, to explain exponential growth and the lack thereof during the stationary phase.

Balanced growth is the relatively intuitive idea that in order for cells to accumulate at an exponential rate, the underlying biomass-generating processes must occur at balanced rates. A constant population doubling rate arises as a result, because cells contain the processes required to make more cells, so the rate of accumulation is proportional to the population size. Conversely, if a material constraint prevents the internal rates from being balanced, growth is halted. This may occur, for example, if the cells consume the nitrogen in the growth medium to below a certain concentration relative to the available carbon. Thus, balanced growth neatly explains the stationary phase as being due to the depletion of a limiting nutrient component such that some processes required to make more cells cannot operate in balance.

Ultimately, balanced growth is a mathematically simple statement at the macroscale captured by Eqs. (1) and (2), yet its simplicity belies the extraordinary chemical complexity operating in the background. It requires the immensity of cellular regulation and adaptation to operate in concert to ensure that every constituent in the cell doubles at the same rate, despite these constituents having vastly different compositions. After Campbell, balanced growth was no longer seen as a characteristic of one of the many growth phases through which bacteria must pass. Rather, it was understood as a steady state that could be maintained by dilution, in theory for as long as an investigator wishes, because the addition of fresh media could ensure that media components are always provided in excess. According to Schaechter, "the difference between 'exponential phase' and 'balanced growth' is the difference between watching apples fall and thinking of gravity [3]."

As such, balanced growth has become the standard condition in which bacterial physiology is studied. The growth rates (and other parameters [4]) measured in balanced growth conditions (Box 1) are robust and reproducible, exhibiting less than 5% variability from day-to-day or laboratory-to-lab. From an analytic perspective, balanced growth implies that, on average, all the relative synthesis rates in the cell are uniquely defined by the macroscale doubling rate: if the number of cells doubles once per hour, so too does the mass of DNA, RNA, and protein. These relative synthesis rates can be converted to absolute rates if the population averaged abundance of a particular constituent is known at a particular doubling rate. For example, Bremer and Dennis [4] report that the protein content of *E coli* B/r growing at one doubling per hour is 8.7×10^8 amino acids per cell, which necessitates a peptide polymerization rate of 1.45×10^7 amino acids per minute. This example highlights the power of the idea of balanced growth, as it allows for the quantification of a complex, microscale process (amino acid polymerization) from a small number of readily accessible macroscale observables (growth rate, total protein content).

In this tutorial, we will explore the consequences of balanced growth for mathematical models of bacterial growth physiology. Applied to individual metabolic reactions in the cell, balanced growth implies a sum rule for reaction rates (or *reaction flux*) that is analogous to Kirchhoff's current law. Remarkably, the analogy with electrical network analysis extends beyond this—empirical relations governing protein concentration per cell and the rate of enzyme-catalyzed reactions yield constraints analogous to Kirchhoff's voltage law and Ohm's law. Overall, balanced growth leads to an "Ohmics" framework that quantifies the coupling between bacterial physiology, metabolic rates, and protein expression in *E coli*. The impact of this framework is described across the six remaining sections in this tutorial. In Sec. II, a common and powerful tool in bacterial network analysis, flux balance analysis (FBA), is summarized. Enzyme kinetics are developed in Sec. III as a basis for understanding subsequent sections. Then the concept of a constraint on the total protein in a cell is introduced in Sec. IV, and the power of such constraints in coarse-graining the proteome is demonstrated in Sec. V. Finally, some examples of applications of proteomic coarse-graining are presented in Sec. VI.

Box 1: Quantifying *Escherichia coli* growth

E. coli has several useful characteristics that make it an ideal model organism: its nutritional demands are simple, its optimal growth temperature is commensurate with our own, and its growth timescale is comparable to a reasonable workday.

At the least, *E. coli* requires a nutrient environment with plentiful carbon (*e.g.* glucose) and nitrogen (*e.g.* ammonium chloride), and a buffer to neutralize metabolic waste products. The gold standard for reproducible growth of *E. coli* is the morpholinopropane sulfonate (MOPS)-buffered medium developed by Neidhardt [5]. As a gut-dwelling bacterium, *E. coli* grows most rapidly at 37 °C with an unrestricted supply of oxygen. To ensure a constant temperature, bacteria are typically grown in a flask or test tube immersed in a water bath shaker. Aeration is maintained by turbulent mixing of the medium as the culture vessel shakes, and the volume of the liquid medium is kept low to maximize the rate of oxygen transfer.

A convenient method for monitoring the growth of bacterial cultures is to measure the degree to which cultures *scatter* light using a spectrophotometer. Over a narrow range of number density, the fraction of scattered light – corresponding to apparent *absorbance* – is proportional to the number density of the particles scattering light. Typically, light scattered at 600 nm (sometimes called the *optical density* at 600 nm, or the OD_{600}) is used as a proxy for cell number density. In the dilute limit, where multiple scattering events are negligible, the ratio of the incident (I_0) to transmitted (I_f) light intensity is related to the number of bacteria N by,

$$OD_{600} = \log \frac{I_0}{I_f} = \ell N Q(\lambda),$$

where ℓ is the path length over which scattering occurs, and Q is a shape parameter that depends upon the size and shape of the light-scattering particles and the wavelength of the incident light. In a given spectrophotometer cuvette, the volume of the scattering chamber is fixed (*i.e.* ℓ is constant), and so *provided the average size and shape of the bacteria remains constant over the experiment*, the optical density provides a convenient proxy for changes in number density. There are several practical points to consider:

(1) In balanced growth, the cell population increases exponentially in time. The $\log_2$ of the number density (or a suitable proxy such as the OD_{600}) plotted against time produces a straight line, the slope of which is the doubling rate μ. In practice, the linearity of the data is extraordinary, and one should expect a coefficient of determination $r^2 > 0.995$.

(2) The measured optical density will vary from spectrophotometer-to-spectrophotometer. If absolute number density is required, then the optical density must be calibrated against true number density (obtained through plating dilutions of the growth culture and counting colonies). This calibration must be redone whenever there is a possibility that the shape parameter Q has changed.

(3) In Sec. III, the fact that average cell size changes dramatically with growth rate will be discussed. This results in much lower optical density measurements of slowly growing cells compared with faster growing cells at the same number density.

(4) Reading optical density of cultures in microwell plates posses several practical challenges: evaporation can lead to path length changes throughout the experiment, incomplete agitation and cell clumping can result in a scattering volume that is not representative of the individual bacterium, and scratches on the plate may produce spurious scattering. As such, unless the microplate growth is carefully calibrated [6], it is recommended that optical density measurements be made in a non-disposable cuvette mounted in a spectrophotometer.

II. FLUX BALANCE AND KIRCHHOFF'S CIRCUIT LAWS

A. Background

It has been widely appreciated since before the advent of balanced growth as a concept that cells use internal chemical reactions to assimilate material from the environment and reconstitute it in specific ratios corresponding to their overall chemical composition, which shows very little cell-to-cell variation. That is to say that growth rate, as observed, emerges in part from the sum of the chemical reactions which occur in cells (the other part is management of transcription and translation, discussed in Sec. V). In this context, balanced growth requires that metabolic reaction rates themselves be balanced such that they can generate the components of biomass in the specific ratios required to make more cells, and the energy required to power reconstitution of these components.

The idea that metabolic reaction rates must be balanced in steady-state growth conditions was first applied to metabolic characterization by Papoutsakis in 1984 [7], in a forward-thinking study of microbial fuel production, and arguably formalized a decade later by Varma and Palsson [8]. Significant contributions were made throughout this period by several researchers in related fields, and the development of the resulting "flux balance analysis" (FBA) methodology has occurred organically and informally. Today, various forms of FBAs exist and are standard, highly tractable tools to predict growth rates, metabolic flux distributions, and engineering strategies for biomanufacturing (Box 2).

Understanding FBA first requires an understanding of what is meant by *flux* in a metabolic context. As in other areas of study, flux in metabolism is a normalized rate; it is a measure of how quickly molecules are transformed by enzyme catalysts. Whereas other forms of flux, such as magnetic field flux, are normalized to a flow-through area, metabolic flux is instead normalized to biomass. It typically has dimensions of concentration of molecules transformed per unit mass of biomass per unit time, with standard units of millimoles-per-gram dry weight of biomass-per-hour (mmol $\mathrm{gCDW^{-1}\,h^{-1}}$).

Every reaction in metabolism can be described as carrying some amount of flux (which may be 0 mmol $\mathrm{gCDW^{-1}\,h^{-1}}$), and the boundary of metabolism is defined by import and export fluxes, which capture the rates at which material is taken up from the environment and wastes are exported to the environment, respectively. When metabolism is considered as a collection of chemical reactions, it is clear that even simple organisms are powered by a complex network made up of overlapping, branching, and cyclical structures (Fig. 1). Material flows through this network according to rates described by reaction fluxes, much like electric current flows through circuits. Despite the high degree of complexity that is possible in metabolic reaction networks, some core structures have persisted throughout evolutionary history. For example, central carbon metabolism, in which most of the energy and chemical backbones required to make more cells are produced, is highly conserved across all branches of the tree of life.

B. Flux balance as a linear programming problem

In flux balance analysis (FBA), the principle of balanced growth—and balanced fluxes—is applied to significantly simplify analysis of complex metabolic networks. This simplification begins with mass balances on each of the metabolites, x_i, in metabolism:

$$\frac{dx_i}{dt} = \sum_{j=0}^{n} \alpha_{ij} v_j - \sum_{k=0}^{m} \beta_{ik} v_k, \tag{3}$$

where the α_{ij} and β_{ik} capture stoichiometry of the n producing and m consuming reactions of metabolite x_i, respectively, operating at rates v_i and v_k. These balances can be expressed more compactly—and more usefully—in matrix form:

$$\frac{d\vec{x}}{dt} \equiv \vec{j} = \mathbf{S} \cdot \vec{v}, \tag{4}$$

where $\vec{x}$ is the vector of metabolite concentrations, and the time-rate-of-change is called the *flux* $\vec{j}$ expressed in terms of the *stoichiometric matrix* $\mathbf{S}$ and the *rate vector* $\vec{v}$.

The stoichiometric matrix, $\mathbf{S}$, is a critical component of FBA and all other related *constraint-based* modeling approaches. Its rows correspond to metabolites and columns to the reactions in which they participate, with entries reflecting

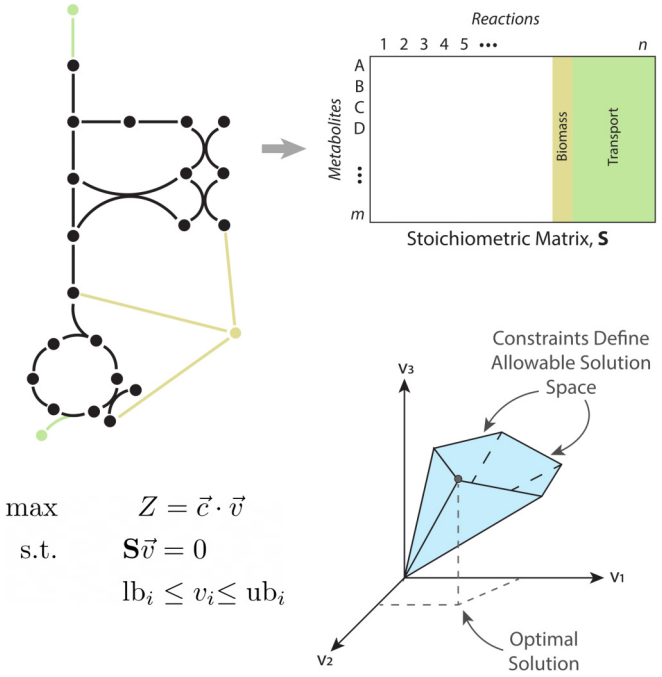

FIG. 1. FBA summary. Metabolism is a complex network of interrelated chemical transformations that interact with the environment via transport reactions (green) and ultimately produces the material and energy required to make more cells (yellow). In FBA, the wiring of metabolism is captured in an $m \times n$ stoichiometric matrix $\mathbf{S}$, which is always rectangular because of the biomass reaction and transport reactions. A constrained optimization is used to find rate distributions $\vec{v} \in \mathbb{R}^n$ for a given objective function Z. The constraints delimit an admissible solution space in $\mathbb{R}^n$, and the optimal solution is found by solving the constrained optimization problem. Figure inspired by [14].

the stoichiometry of these reactions. For a reaction network with m metabolites and n reactions, $\mathbf{S}$ has dimensions of $m \times n$. An example stoichiometric matrix might look like

$$\mathbf{S} = \overbrace{\begin{bmatrix} 0 & 0 & -1 & 1 & \cdots & 0 \\ -1 & 0 & 0 & 2 & \cdots & 1 \\ \vdots & \vdots & \vdots & \vdots & \ddots & \vdots \\ 0 & 0 & 0 & 0 & \cdots & -1 \end{bmatrix}}^{\text{Reactions}} \Bigg\} \text{Metabolites} \tag{5}$$

The stoichiometric matrix is like a metabolic wiring diagram. It captures how fluxes can move material through the metabolic network, regardless of other factors such as metabolite or enzyme concentrations, or thermodynamics. The structure of the stoichiometric matrix provides the most fundamental *constraint* on fluxes in the metabolic network because the stoichiometry of a given reaction can never be changed. This is similar to how a circuit wiring diagram describes the constraints on how electricity can flow through a circuit. Of course, as with an electric circuit, determining the actual flows through the metabolic networks requires more knowledge than just the structure.

At steady state, for example during balanced growth, Eq. (4) becomes

$$\frac{d\vec{x}}{dt} = \vec{j} = \mathbf{S} \cdot \vec{v} = 0. \tag{6}$$

Thus, the problem of finding the values of metabolic fluxes which yield balanced growth is equivalent to solving a homogeneous system of linear equations. In real metabolic networks, this problem is always *underspecified* because there are always more reactions than there are metabolites: $m < n$. Underspecification is guaranteed by the fact that metabolism is an open system, with import and export reactions. This condition ensures that at least one metabolite participates in multiple, unbalanced reactions (Fig. 1). Indeed, in real metabolism, there are typically multiple metabolites which participate in transport reactions. Furthermore, cycles and other complex structures are guaranteed to yield an underspecified system in Eq. (6). Moreover, most metabolites participate in just a few reactions, leading to a *sparse* stoichiometric matrix, which poses specific challenges to the computational tractability of solving Eq. (6).

To address the challenge of underspecification, the problem of finding fluxes, $\vec{j}$, in balanced growth can be recast as a *constrained optimization* via the application of two principles: first, that metabolism has been optimized to achieve a specific function, described by a linear combination of fluxes; and second, that many rates in the metabolic networks are *bounded* by some observable value. For example, the rate of carbon import sets upper bounds on all downstream fluxes, and nonzero growth rate ($\lambda > 0$, i.e., cells are alive) requires that some critical fluxes, such as those which generate energy, be nonzero. These principles yield the following *constrained optimization formulation*:

maximize the objective function

$$Z = \vec{c} \cdot \vec{v} \text{ (often the growth rate} = \lambda), \tag{7}$$

under balanced growth conditions $\vec{j} = \mathbf{S} \cdot \vec{v} = 0$, (8)

subject to physical constraints on the rates $\mathrm{lb}_i \leqslant v_i \leqslant \mathrm{ub}_i$. (9)

Here the *objective function*, Z, is a linear combination of some fluxes in the metabolic network. The vector $\vec{c}$ is made up of user-defined weights that must be chosen such that Z corresponds to this desired linear combination of fluxes. Individual rates in the network have lower and upper bounds (lb_i, ub_i) which must be specified. Typically, bounds are used to capture measured import and export fluxes. Various algorithms exist to rapidly solve this optimization problem; see Box 2 for more information.

The baseline assumption in FBA is that the objective function, Z, is proportional to the growth rate, λ, based upon the intuitive idea that evolution has selected for cells that grow as quickly as possible. Cell proliferation emerges from many fluxes acting in concert to produce the components of biomass. As such, metabolic network models include a *pseudoreaction* representing biomass accumulation, typically

derived empirically through measurement of the elemental composition of biomass, the waste products, and energy requirements of producing a new cell. The rate of the resulting so-called "biomass reaction" has units of grams of cell dry weight-per-hour, such that when it is normalized as a flux, it yields units of gCDW gCDW^{-1} h^{-1} = h^{-1} and corresponds to the growth rate of the cell for a given flux distribution.

C. Fluxes are currents of chemical mass

In the same way that electric current is the flow of electrons through a conducting material, metabolic flux is the flow of chemical mass through enzyme-catalyzed reactions. Conservation of mass and energy applies to both systems, so that the flux entering and exiting a junction, or branch point, must balance. The stoichiometry matrix **S** is sparse [Eq. (5)] and the overall flux-balance condition [Eq. (4)] applies to each metabolite. Focusing on the mth metabolite,

$$\sum_{\text{node } m} S_{mn} v_n = \sum_{\text{node } m} j_n = 0, \tag{10}$$

where the flux $j_n = S_{mn} v_n$ is the product of the reaction stoichiometry and the reaction rate for all reactions leading in and out of metabolite m,

$$\vec{j} = \mathbf{S} \cdot \vec{v} = \vec{0} \Longleftrightarrow \sum_{\text{node } m} j_n = 0$$

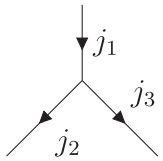

Equation (10) is the metabolic analogy of Kirchhoff's current law, as it expresses how balanced growth imposes flux conservation at each junction in the network. The solution to the flux-balance condition, Eq. (6), is the *nullspace* of the stoichiometric matrix, **S**.

Metabolic networks are not exclusively unidirectional—there are cycles or loops that are associated with conserved chemical scaffolds. For example, energy-carrying molecules are routinely used in reduction-oxidation [NAD(P)H ↔ NAD(P)+] or phosphorylation/dephosphorylation (ATP ↔ ADP) cycles to couple energy transfer between metabolic reactions. Conserved quantities—the backbones that are cycled through loops in metabolism—are determined by the *left nullspace* of the stoichiometric matrix instead. The left nullspace is simply the nullspace of the transpose of a matrix, so the conserved quantities in a metabolic network $\vec{u}$ can be found by solving the equation

$$\mathbf{S}^T \cdot \vec{u} = 0. \tag{11}$$

Specific conservation relationships can be found using the column vectors, $\mathbf{s}_j$, of the stoichiometric matrix and the basis vectors of its left nullspace:

$$\sum_i s_{ij} u_i = 0. \tag{12}$$

Whereas the only flow in electrical circuits is of electrons, there are many unique flows of chemical species in metabolic networks. As such, many cycle-conservation relationships exist. Enumerating these can be useful to characterize metabolic pools necessary to maintain steady states.

Box 2: Flux Balance Analysis (FBA) in a Nutshell

FBA is a highly tractable method of estimating flux distributions that can be performed on most personal computers using standard packages and solvers available for MATLAB [9], Python [10], and Julia [11]. FBA can be performed on any reaction network, but is generally used with *genome-scale metabolic models* (GEMs), which are reconstructions of metabolisms from the genome sequence(s) of specific organisms. They may additionally integrate other information beyond genome sequences, such as transcriptomics. Many GEMs are available via public repositories such as the Biochemical, Genetic and Genomic (BiGG) knowledge base [12], and the quality of GEMs is ensured with the MEMOTE framework [13].

The basic premises of FBA are twofold: first, that cells have evolved to optimize some objective function, typically growth rate, given some bounds on uptake fluxes; and second, that the stoichiometries of chemical reactions provide constraints within which fluxes yielding an optimal solution to this objective must fall. Together, these yield a linear programming problem with a solution that falls within a high-dimensional cone. Typically, solutions are projected onto a two-dimensional space for interpretation. See Fig. 1 below for a visual explanation of the basis of FBA.

Many other constraint-based methods have been developed as expansions and/or modifications to FBA. Some of these which are commonly used are summarized below, with relevant literature cited for further exploration:

(1) **Dynamic FBA (dFBA)** [15]. A fundamental assumption of standard FBA is that cells operate at steady-state. This is only truly valid for continuous cultures or for a short period in mid-exponential phase for batch cultures. In dFBA, quasi-steady state is assumed for small time intervals over the course of a batch culture. The flux distributions determined by FBA for each time interval are used to update external concentrations based on an assumption of linearity over this time period. The updated external concentrations at the end of the interval are used to initiate a new FBA calculation for the next interval. In this way, a linear programming approach can be used to estimate nonlinear growth characteristics.

(2) **Flux Variability Analysis (FVA)** [16]. In FVA, the maximum and minimum value for all fluxes which can support some fraction of the optimal value of the objective function are determined. This requires a *bi-level* optimization approach and can uncover robustness in metabolic networks by determining which fluxes can vary without significantly affecting the objective.

(3) **Parsimonious FBA (pFBA)** [17]. In exponentially growing cultures, it is reasonable to assume that fast growers will be selected for. FBA captures this assumption well, but there is an additional reasonable expectation that among fast growers, cells which use the least amount of enzyme to achieve a given growth rate will outcompete

their neighbours. pFBA uses FVA to find alternatives to solutions found via FBA, and classifies these according to their contribution to the optimal flux distribution, with longer pathways being penalized.

(4) **Elementary Flux Mode Analysis (EFMA)** [18]. Elementary flux modes (EFM) are the minimal functional units of a metabolic network such that every single possible path of a metabolic network can be constructed via linear combinations of EFMs. They essentially capture the routes through which material can flow at steady state, and if any EFM is blocked, its function in the network will also be blocked. This is a lot like sub-circuits in a home electrical system; if a breaker is flipped, power to one room may be disrupted, whereas other rooms in the house will still have current. Enumerating EFMs is computational challenging, but EFMA can be used to find functional modules in metabolic networks, and to determine the robustness of networks to perturbations.

III. BIOLOGICAL CATALYSIS

The majority of protein in the bacterial cell is made up of catalytic molecules called "enzymes." Enzymes carry out the reactions whose fluxes are predicted in FBA. In doing so, they allow otherwise extremely slow reactions to occur on timescales required for life [19]. In some cases, they couple reactions to the breaking of energetic bonds in cofactor molecules such as ATP or NADH to force irreversibility in a particular direction. Cell proliferation rates of tens-of-minutes (or even tens-of-hours) are only possible through the catalytic action of enzymes.

A. Enzyme kinetics

A simple mathematical model for irreversible enzyme catalysis was introduced by Michaelis and Menten [20], and refined by Briggs and Haldane [21]: an enzyme E binds with a substrate S to form an activated complex ES that is converted to the product P (thereby releasing the enzyme E),

$$E + S \underset{k_{off}}{\overset{k_{on}}{\rightleftharpoons}} \underset{\text{complex}}{ES} \xrightarrow{k_{cat}} E + P.$$

Assuming mass-action kinetics, the rates of formation of the concentrations of each species are

$$\begin{aligned}
\frac{d[E]}{dt} &= -k_{on}[E][S] + k_{off}[ES] + k_{cat}[ES], \\
\frac{d[S]}{dt} &= -k_{on}[E][S] + k_{off}[ES], \\
\frac{d[ES]}{dt} &= k_{on}[E][S] - k_{off}[ES] - k_{cat}[ES], \\
\frac{d[P]}{dt} &= k_{cat}[ES],
\end{aligned} \tag{13}$$

and the total enzyme concentration, $[E_{tot}]$, is conserved: $[E_{tot}] = [E] + [ES]$. The object of interest is the rate of product formation, $d[P]/dt$. If the substrate abundance far exceeds the enzyme abundance, $[S] \gg [E]$, then the complex concentration $[ES]$ does not change on the timescale of product formation,

$$\frac{d[ES]}{dt} = k_{on}[E][S] - k_{off}[ES] - k_{cat}[ES] \approx 0.$$

From the conservation of the total enzyme concentration, $[E] = [E_{tot}] - [ES]$, the free-enzyme concentration $[E]$ can be eliminated, with the active complex concentration $[ES]$ written in terms of the total enzyme concentration $[E_{tot}]$,

$$\begin{aligned}
[ES](\{k_{off} + k_{cat}\} + k_{on}) &\approx k_{on}[E_{tot}][S] \\
\Rightarrow [ES] &= [E_{tot}]\frac{[S]}{[S] + K_M},
\end{aligned}$$

so that

$$\frac{d[P]}{dt} = k_{cat}\,\frac{[S]}{[S] + K_M}\,[E_{tot}]. \tag{14}$$

The constant $K_M = (k_{off} + k_{cat})/k_{on}$ is called the *Michaelis constant*, and sets a characteristic concentration scale for the substrate $[S]$ at which the rate of product formation is half-maximal. The overall rate, $d[P]/dt$, quantifies the flow of molecules of S through a reaction in a given time in much the same way that, for example, electric current is a measure of charge flux in a wire.

The derivation presented here is that of Haldane. It differs from the earlier Michaelis-Menten derivation insofar as there is no assumption that any of the kinetic steps are rapid (the *quasi-steady-state approximation*), only that the abundance of the substrate far exceeds the abundance of the enzyme, which is a less restrictive assumption in most applications. The conditions under which the Michaelis-Menten expression, Eq. (14), is a valid approximation of real enzyme mediated kinetics, Eq. (13), continues to be an active area of research [22].

Not all enzyme-catalyzed reactions are irreversible, or proceed in a single step [23]. Nevertheless, the simple irreversible case illustrates three fundamental control points by which flux through enzyme-mediated reactions may be modulated. Of the three factors on the right-hand side of Eq. (14), the first two control flux via enzyme *activity*, whereas the third controls flux via enzyme *abundance* (Fig. 2). Notice that the substrate saturation dynamically partitions the total enzyme abundance $[E_{tot}]$ into a flux-carrying "active" fraction $[\Delta E]$,

$$\text{flux} = k_{cat}\,\frac{[S]}{[S] + K_M}[E] \equiv k_{cat}\,[\Delta E], \tag{15}$$

and a non-flux-carrying "free" fraction $[E_0]$ [24],

$$[E_{tot}] = [E_0] + [\Delta E] \equiv \underbrace{\frac{K_M}{[S] + K_M}\,[E_{tot}]}_{[E_0]} + \underbrace{\frac{[S]}{[S] + K_M}\,[E_{tot}]}_{[\Delta E]}. \tag{16}$$

Combining these two equations, Eqs. (15) and (16), the flux and the total enzyme concentration $[E_{tot}]$ are related as

$$[E_{tot}] = [E_0] + \frac{\text{flux}}{k_{cat}}. \tag{17}$$

This expression will be particularly relevant in the next section.

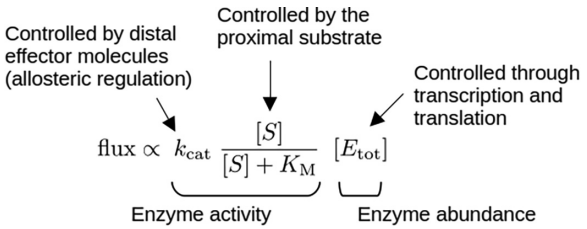

FIG. 2. Control of enzyme-mediated flux. The catalytic rate, k_{cat}, can be modulated by cofactors (including metal ions, vitamins, and nucleoside triphosphates) or by small-molecule regulators. Modulation by distal small molecules is called *allosteric regulation* [25], and it allows the tuning of enzyme activity via signals from other parts of the reaction network. The enzyme activity is also responsive to the substrate concentration relative to the Michaelis constant, $[S]/K_M$, with $[S]/K_M \approx 2$ for most enzymes in *E coli* [24]. Finally, the flux can be adjusted via transcriptional and translational control of the enzyme protein abundance $[E_{tot}]$ [26]. Although not all enzyme-mediated fluxes respond to allosteric control, most respond to changes in substrate availability and changes in enzyme abundance.

B. Ribosomes catalyze protein synthesis

Enzymes, like all proteins, are made up of polymerized amino acids. *Ribosomes* are a special biological catalyst responsible for carrying out amino acid polymerization to make all proteins [27]. As they are themselves in part made up of proteins, ribosomes are required to make more ribosomes. They also contain catalytic ribonucleic acid (RNA), and they are therefore *ribozymes*. Although enzyme abundance and activity are typically the focus of metabolic network models, ribosome abundance exhibits strong growth rate dependence [4,28], and under conditions of rapid growth or inhibition by ribosome-targeting antibiotics, ribosome-affiliated proteins can occupy 30–50 % of the total protein mass [26,29,30].

The catalytic activity of ribosomes shares many of the same features as the Michaelis-Menten scheme detailed in Sec. III. They use the amino acids carried by charged transfer RNAs (tRNA) as substrates to produce an elongating *polypeptide* chain. In effect, the translating ribosome is an enzyme that converts charged tRNA into uncharged tRNA (Fig. 3). The kinetic scheme that results is analogous to that used to arrive at Eq. (14). As a result, the rate of protein synthesis catalyzed by a ribosome can also be analogously written as [31]

$$\text{rate of protein synthesis} \propto k_{elong} \frac{[T^\star]}{[T^\star]+K_M} [\text{Rb}_{tot}], \quad (18)$$

where $[T^\star]$ is the concentration of charged tRNA, K_M is the Michaelis constant associated with the reaction, and $[\text{Rb}_{tot}]$ is the total concentration of ribosomes.

As is the case with metabolic enzymes, the rate at which ribosomes operate is dependent on kinetic and saturation factors, and the total ribosome concentration. Also like metabolic enzymes, their activity may be modulated via changes to activity and/or changes to abundance. The *flux* they carry is the rate of protein synthesis per unit time; this rate is a critical factor in the synthesis rate of biomass, as will be elaborated on in the next section. Ribosomes in fast-growing cells tend to operate very close to saturation, and the rate at which they bind tRNA is nearly diffusion-limited [31]. That is to say, they typically operate close to the maximum possible capacity defined by physical constraints in exponentially growing microbes.

During exponential growth, the fluxes carried by metabolic enzymes and by ribosomes, including the synthesis of new ribosomes, are all in balance. In both cases, rates depend directly on the abundance of the corresponding enzymes, which share a precursor pool of amino acids. In the next section, the consequences of this in the context of a total protein constraint will be discussed.

IV. CONSTRAINTS ON PROTEIN EXPRESSION

Microbes can maintain balanced growth over a wide range of conditions, including in the presence of sublethal antibiotic concentrations, in conditions of osmotic stress, or even in temperatures outside the optimal range. In suboptimal environmental conditions, cells still achieve exponential growth, but with reduced growth rate, $\mu < \mu_{max}$. This is possible because different metabolic subnetworks are active in different nutrient and/or environmental conditions. Exquisite control strategies have evolved to modulate the expression and

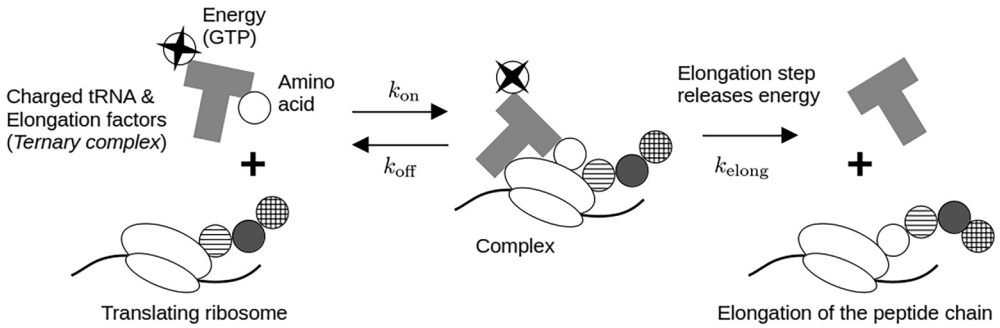

FIG. 3. Ribosomes are catalysts that make proteins. Ribosomes use transfer RNA (tRNA) molecules carrying specific amino acids as a substrate. The tRNA, along with an energy source in the form of guanosine triphosphate (GTP), binds to the active ribosome to form a complex. The GTP is hydrolyzed to release energy required to form a new peptide bond, resulting in an elongated polypeptide. Many elementary steps are involved in ribosomal catalysis, but these can be lumped into three steps to yield similar kinetics to those of metabolic enzymes: (1) formation of a complex, with rate constant k_{on}, (2) dissolution of the complex, with rate constant k_{off}, and (3) formation of a peptide bond and concomitant release of the uncharged tRNA, with rate constant k_{elong}. Figure reproduced from [31].

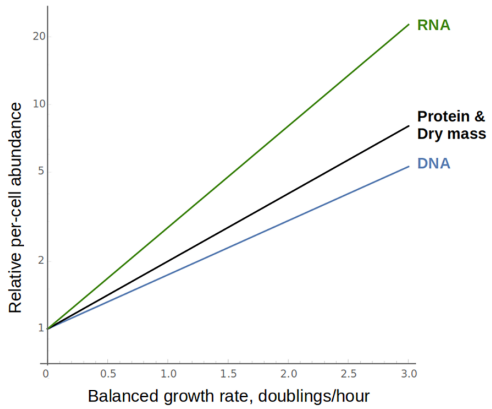

FIG. 4. Microbial physiology is intrinsically linked to growth rate. In bacterial cultures in balanced growth, cellular composition is uniquely defined by growth rate: on a per-cell basis, the RNA, protein, and DNA masses all grow exponentially with growth rate.

activity of metabolic enzymes to balance rates even in sub-optimal conditions, and the discovery and elucidation of the molecular mechanisms underpinning such regulation continues to be an active research stream.

In what has been described as the "fundamental experiments of bacterial physiology" [32], Maaløe and collaborators used this consistency of balanced growth to deliberately vary the growth rate of exponentially growing microbial cultures through environmental manipulation. They found that the size and macromolecular composition of *Salmonella* cells exhibit a characteristic growth rate dependence [33]. The average cell volume increases roughly exponentially with growth rate, approximately as 2^{μ} [34]. Consequently, cells growing with a doubling time of 20 min are twice as large as those doubling every 30 min, and four times as large as those doubling every hour. Furthermore, irrespective of the chemical details of the growth medium, the per-cell abundance of RNA, DNA, and protein also exhibit an approximately exponential dependence on μ (Fig. 4),

$$\text{DNA-per-cell} \propto 2^{0.8\mu}, \quad \text{protein-per-cell} \propto 2^{\mu},$$
$$\text{RNA-per-cell} \propto 2^{1.5\mu}. \tag{19}$$

Since the per-cell protein amount and cell volume increase with approximately the same growth rate dependence, the protein concentration in cells exhibits little variation (<5%) over most nutrient conditions [35,36].

Thus, even though cells must—and do—express different enzymes in different environmental conditions to maintain balanced growth, the protein content of those cells remains approximately the same. This means that if the expression of one group of proteins is upregulated to increase the concentration of those proteins, then the concentration of other proteins must necessarily decrease to accommodate the change. For example, if expression of the proteins required for glucose assimilation is upregulated due to the presence of glucose in the environment, then the concentrations of proteins required to assimilate other carbon sources must decrease in response. The empirical constancy of protein concentration provides a strong constraint on protein expression in many microorganisms [37], but it has been best studied in *E coli* [38].

A. Growth-dependent macromolecular composition

Box 3: Balanced growth in sub-optimal conditions

Bacteria have a preferred carbon source with which they can generate more biomass most rapidly, but they may still achieve balanced growth at sub-optimal rates in media containing carbon sources of reduced nutritional quality, provided that other nutrients such as nitrogen are present in sufficient excess. Microbial growth rates can also be directly modulated by growing cells in continuous cultures, in which the rate of culture replacement defines the rate at which cells must grow to remain.

Maaløe and colleagues used these two approaches to control the growth rate of fast-growing *Salmonella* cultures by growing them on a wide range of culture media and in continuous cultures with varied dilution rate [33]. They then examined the relationships between various physiological features of the cells in their cultures and the growth rates of those cultures. Cell size, protein mass, RNA mass, and DNA mass per-cell were measured very carefully, and, remarkably, it was found that these physiological parameters all scaled exponentially with the doubling rate, μ [Eq. (19), and Fig. 4].

In fast-growing microbial cells, a doubling in growth rate yields almost 3 times as much RNA per cell, for example. Maaløe and colleagues showed that this relationship was true in both batch cultures, in which nutritional quality controlled growth rate, and in continuous cultures in which growth rate is controlled by the culture dilution rate.

B. Global constraints on protein expression

This total protein constraint can be simply expressed by substituting *protein mass fraction* in place of *concentration*. These are proportional as long as the per-cell protein concentration remains invariant [38]. If the protein mass fraction of protein i is ϕ_i, then the total protein constraint is expressed as

$$\sum_i \phi_i = 1. \tag{20}$$

Thus, if the mass fraction of one protein increases, there must be a concomitant decrease in the mass fractions of one or more other proteins.

In *E coli*, there is an empirical connection between the enzyme-mediated reaction flux, the balanced growth rate, and the *total* enzyme mass fraction under a large range of growth conditions. The mass fraction of a given set of catalytic proteins, ϕ_i (which includes metabolic enzymes and ribosomal proteins), is often found to be a *linear* function of the growth rate λ [26,30,36],

$$\phi_i = \phi_i^0 + \frac{\lambda}{\kappa_i}. \tag{21}$$

The total flux through reactions that are active in a given set of conditions is often directly proportional to the growth rate, λ [8]. Comparison of Eq. (21) to the equation for irreversible enzyme kinetics [Eq. (17)] then provides a possible interpretation of the phenomenological parameters ϕ_i^0 and κ_i [24,39]: the former is the mass fraction of non-flux-carrying protein

that arises because enzymes may not operate at saturation, while the latter is a measure of the catalytic turnover of the active fraction.

Rearrangement of Eq. (21) yields an expression for growth rate in terms of the active protein fraction:

$$\left(\phi_i - \phi_i^0\right) = \lambda\left(\frac{1}{\kappa_i}\right). \tag{22}$$

Here, the relationship is written to show that a rate, λ, multiplied by a factor capturing resistance to flux, $1/\kappa_i$, is equivalent to a potential—the flux-carrying portion of the protein mass fraction. This is mathematically and conceptually equivalent to Ohm's law, $V = iR$, in which a potential (V) is equivalent to the product of a flux (i) and resistance thereto (R).

Essentially, in analogy with electrical circuit elements, the protein cost associated with a particular enzyme-mediated reaction ϕ_i has the form of a battery (ϕ_i^0) in series with a resistor ($1/\kappa_i$), where the battery is always oriented to oppose the flow of current (λ):

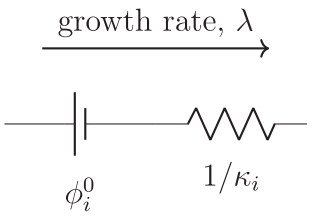

The remainder of this tutorial explores the consequences of this linear empirical relationship, along with other constraints that are active during balanced growth—flux balance at reaction nodes [Eq. (10), elaborated in Sec. II] and the total protein constraint [Eq. (20)]. Together, these yield a framework for quantifying microbial physiology that is mathematically identical and conceptually analogous to Kirchhoff's circuit laws and Ohm's law under the following associations:

Electrical variables		Physiological variables	Electrical constraints	Physiological constraints
current i	reaction flux j_i ⇔	growth rate λ	Kirchhoff's junction rule	$\sum_{\text{node } m} j_n = 0$ Eq. (10)
voltage V		protein mass fraction ϕ_i	Kirchhoff's loop rule	$\sum_i \phi_i = 1$ Eq. (20)
conductance $1/R$		catalytic constant κ_i	Ohm's law	$(\phi_i - \phi_i^0) = \frac{\lambda}{\kappa_i}$ Eq. (22)

A remarkable feature of networks composed of batteries and resistors is that they can be coarse-grained into smaller equivalent networks, again composed of only batteries and resistors. In the analogy with enzyme kinetics and bacterial physiology, this coarse-graining is tantamount to replacing large subsets of the metabolic network with a single effective enzymatic reaction characterized by two effective phenomenological parameters, the non-flux-carrying offset ϕ_i^0 and the effective catalytic constant κ_i. In the next section, the origin and consequences of this coarse-graining scheme are outlined.

V. NETWORK EQUIVALENCE AND PROTEOMIC COARSE-GRAINING

Bacterial growth and proliferation is driven by a large and complex network of enzyme-catalyzed reactions. Analysis of this network is greatly simplified by the existence of a pervasive hierarchical assembly of modules. A quantitative analogy with electrical circuit analysis can be applied to this modular design that provides a framework for coarse-graining the complex network into empirically determined large-scale modules, a framework called "Ohmics" [40].

A. Bow tie topology and one-port networks

Many complex systems, both arising naturally or engineered synthetically, exhibit common principles of

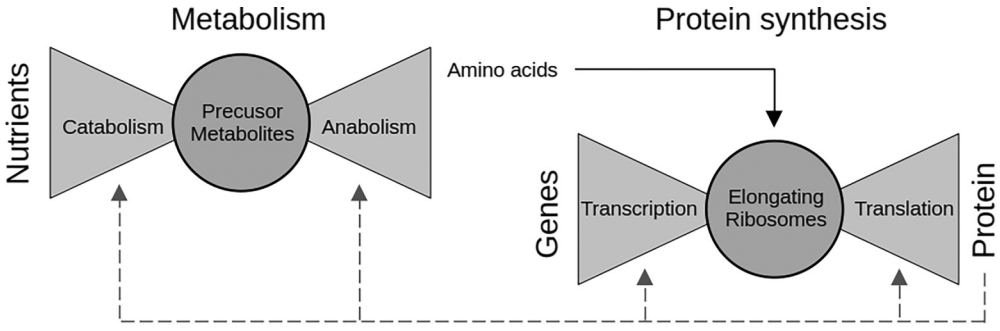

FIG. 5. Bacterial metabolism and protein synthesis exhibits recurrent "bow tie" architecture, typified by diverse inputs canalized toward an intermediate "knot" of precursors that are used to synthesize a diversity of outputs. In the case of metabolism, catabolic enzymes break down environmental nutrients into approximately a dozen different precursor metabolites that are used by anabolic enzymes to synthesize a variety of molecules, including amino acids. Similarly, the transcriptional machinery converts diverse genetic sequences into a pool of 22 different elongating ribosomes that translate these genes into a diversity of proteins, consuming the amino acids produced by metabolism. The synthesized proteins feed back into each module (dashed arrows), creating an autocatalytic loop that defines cellular proliferation. These large-scale topological features are conserved among micro-organisms, although the regulatory strategies used to coordinate modules exhibit considerable variation among species. Redrawn after Csete and Doyle [42].

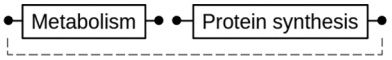

FIG. 6. The modular architecture of metabolism and protein synthesis suggests a simple coarse-graining of the autocatalytic loop underlying bacterial proliferation.

composition [41–43]. Chief among these is a "bow tie" architecture that recurs throughout the network. In bacteria, for example, external nutrients are broken down via catabolism into a pool of a dozen precursor metabolites, and these precursors "fan out" to feed biosynthetic anabolic reactions [44]. Some of these biosynthetic products, including amino acids, then feed a second "bow tie" that converts genetic information into protein via a "knot" of translating ribosomes (Fig. 5).

There are several advantages conferred by a modular bow tie design. The central "knot" provides a natural control point to exert regulation of large-scale flux through the network. Moreover, the material feeding the "knot" can be swapped in or out between species via horizontal gene transfer, making this design both robust and evolvable [42,45,46].

The unidirectionality implied by the "bow tie" metaphor tends to obscure the essential feature of microbial proliferation—bacterial metabolism is an autocatalytic loop, with protein catalysts assimilating nutrients from the environment to create more of themselves [43,47,48] (Fig. 5, dashed arrows). The electrical circuit analogy to a modular, bow tie network is the series assembly of one-port networks (Fig. 6), connected in a closed loop to capture the autocatalytic feedback (Fig. 6, dashed line).

This collection of one-port networks is obviously a vast simplification of the complex underlying network, yet it is able to capture large-scale features of protein expression and flux upon shifts in growth conditions of the bacterium [38]. Furthermore, the electrical circuit analogy points to a method by which this coarse-grained representation can be empirically determined using "equivalent circuits."

B. Thévenin equivalent circuits

Helmholtz and Thévenin independently derived what is now called "Thévenin's theorem": a network of voltage sources and resistors, irrespective of the complexity of their interconnections, can be replaced by an equivalent circuit composed of a single equivalent voltage source, V_{th}, and a single resistor, R_{th}. Empirically, V_{th} is determined by the open-circuit potential across the terminals, whereas R_{th} is determined by the short-circuit current flow between the terminals (and application of Ohm's law) (see Fig. 7).

Imagine the simplest bacterial reaction network: a single enzyme catalyzing a single reaction. For most reactions during balanced growth, flux through such a reaction is proportional to the growth rate [8]. The open-circuit potential of the Thévenin circuit in this scenario corresponds to zero growth rate in the Ohmics analogy, which is incompatible with the balanced growth condition. To overcome this limitation, the current through the reaction (i.e., growth rate) is varied instead through manipulation of nutrient quality, and the corresponding linear change in potential (i.e., the protein mass fraction) is measured via proteomics. When protein mass fraction is plotted against growth rate, the zero-growth intercept provides the offset mass fraction ϕ_i^0 and the slope is the inverse effective catalytic constant $1/\kappa_i$.

Surprisingly, this same approach can be applied at the network level. The overall constraint on the protein mass fraction [Eq. (20)] and the decomposition of enzyme protein mass fraction into a flux-carrying resistor and an opposing non-flux-carrying potential provides analogous prerequisites for the application of Thévenin's theorem. Moreover, the modular "bow tie" architecture suggests that serial decomposition is possible.

The earliest example of this type of coarse-graining was the observation by Neidhardt and Magasanik [27] that the total RNA content of the cell, which is proportional to the ribosomal protein mass fraction, ϕ_{R}, exhibits a linear dependence on

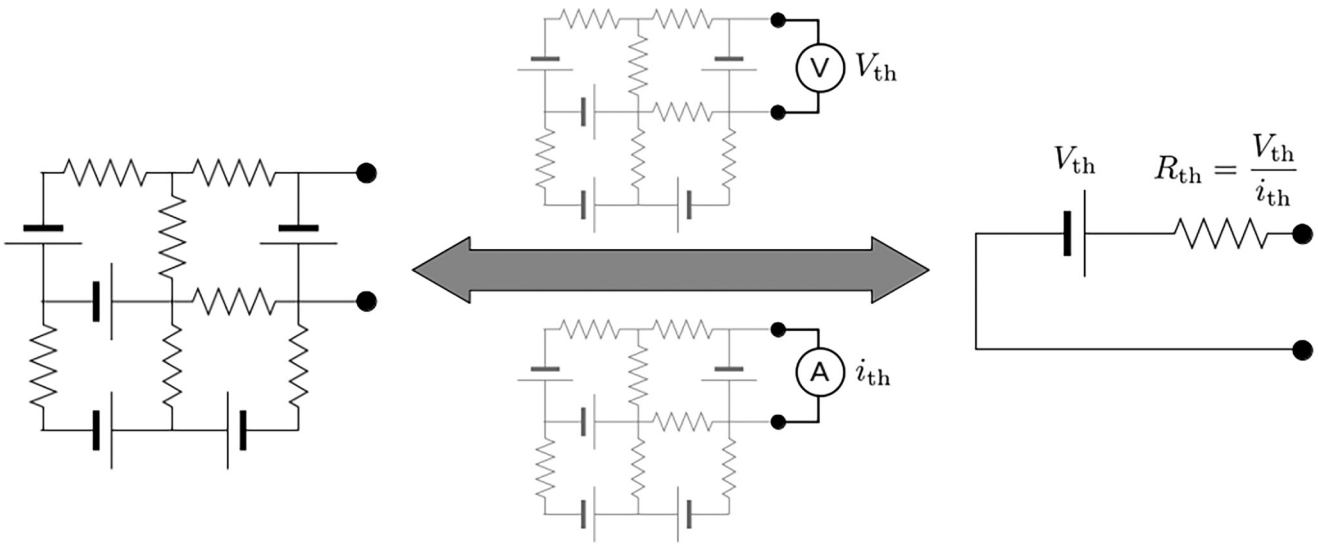

FIG. 7. A useful property of one-port networks composed of resistors and batteries is the coarse-graining afforded by a *Thévenin equivalent circuit*. Irrespective of the topological details, and arrangement of the elements, the network behavior is identical to a single battery (with potential V_{th}) in series with a single resistor (with resistance R_{th}). These elements are determined by the open-circuit potential and the short-circuit current, respectively.

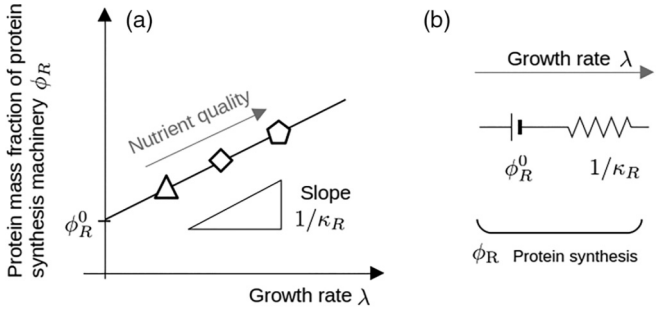

FIG. 8. (a) If the growth rate is modulated via the nutrient quality of the medium (e.g., by changing the carbon source, or supplementing the medium with amino acids), then the mass fraction of proteins responsible for protein synthesis exhibits a positive linear correlation with growth rate [29]—the symbols denote media support slow growth (triangle), moderate growth (diamond), and rapid growth (pentagon). (b) In the electrical circuit analogy, the intercept provides the offset potential ϕ_R^0 that opposes the current, and the slope provides the resistance $1/\kappa_R$.

the growth rate when the growth rate is modulated [Fig. 8(a)]. In the circuit analogy, the inverse slope of this linear relationship is the conductance, κ_R [29], and the zero-growth intercept is the non-flux-carrying offset, ϕ_R^0 [31] [Fig. 8(b)]. It is not difficult to imagine the translational machinery as a fixed catalog of proteins (including ribosomal subunits, initiation factors, elongation factors, etc.; see Table 4 of Ref. [4]) that operate in concert under all growth conditions. But what about a characterization of the heterogeneous, condition-dependent metabolic protein fraction?

1. Anticorrelations among protein sectors

By virtue of the total protein constraint [Eq. (20)], or equivalently Kirchhoff's loop law, it can be inferred that the metabolic protein fraction can be characterized by observing the complementary response of the ribosomal protein fraction, ϕ_R, to decreases in conductance, κ_R (Fig. 9). In *E coli*,

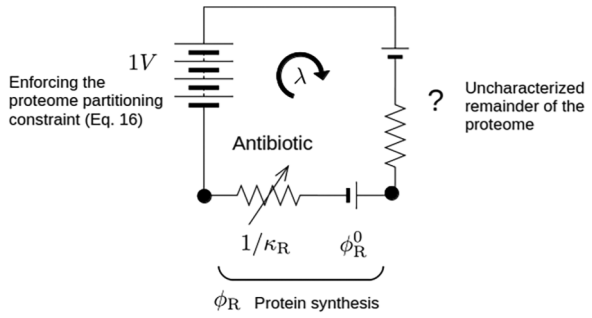

FIG. 9. The constraint on the total protein mass fraction (analogous to Kirchhoff's loop law) provides a simple strategy to infer the coarse-grained parameters characterizing the remainder of the circuit. By modulating the rate of protein synthesis via κ_R, either using a chemical probe like ribosome-targeting antibiotics or a genetic probe like slow-translating mutations to the ribosome, it is possible to modulate the growth rate [29]. As in Fig. 8, tracking the mass fraction of protein-synthetic proteins ϕ_R then provides the resistor and offset associated with the remaining circuit.

antibiotics that target the ribosome (e.g., chloramphenicol, tetracycline, kanamycin) lead to an effective decrease in the conductivity, κ_R, and a commensurate increase in the total mass fraction of the protein synthetic machinery.

Mechanistically, in response to the decrease in protein synthesis flux elicited by the antibiotic, *E coli* synthesizes a small molecule (ppGpp) that upregulates the production of the protein synthetic machinery [49,50]. Empirically, this antibiotic-mediated decrease in κ_R appears to have a negligible effect on the efficiency of metabolic enzymes and so provides a chemical method of modulating κ_R alone. The result is a *negative* linear correlation between the mass fraction of the protein synthetic machinery and the growth rate [Fig. 10(a)].

As with the response of the protein synthesis machinery to changes in nutrient quality (Fig. 8), the slope of the response corresponds to the equivalent conductance, κ_M, through the metabolic part of the circuit, whereas now the zero-growth intercept $\phi_R^{\max}$ corresponds to the total remaining potential after accounting for the offset in the nonribosomal protein fraction, $\phi_R^{\max} = 1 - \phi_M^0$, characterizing the two-module electric circuit analogy that captures the growth-rate dependence of the protein-synthetic machinery under conditions of nutrient change and antibiotic inhibition of ribosome synthesis [Fig. 10(b)].

Other modes of growth inhibition, for example modulation of the carbon uptake, serves to further partition the proteome into modules, or sectors, that respond in concert to the perturbation. In this way, Hui *et al.* [26] created a six-sector coarse graining of the proteome identified as those proteins upregulated in response to inhibition of protein synthesis (R), carbon uptake (C), amino acid biosynthesis (A), both carbon uptake and amino acid biosynthesis (S), in addition to proteins exhibiting growth-rate dependent change in expression but not responding to any inhibitions (U), and proteins exhibiting no growth-rate dependence in expression (O). Figure 11 provides a concise visualization of this empirical decomposition of proteome sectors.

The two-component proteome partitioning (Fig. 10) and the more detailed six-component partitioning (Fig. 11) both illustrate the utility of directed growth-perturbations. For example, in *E coli* the inhibition of protein synthesis [Fig. 10(a); Fig. 11, green arrow] acts like a rheostat (see Sec. VI A), increasing the resistance of the protein-synthetic component of the circuit. As a consequence, the potential drop (i.e., mass fraction) increases across the protein-synthesis resistor, and at the same time the potential drop across all other resistors decreases with the decreasing current (i.e., growth rate). Useful probes of circuit function are those chemical or genetic perturbations that result in the direct increase of one proteome sector and the indirect decrease of all others (Fig. 11, colored arrows).

The proteome fractions ϕ_C, ϕ_S, ϕ_A, and ϕ_U in addition to their shared response to growth-perturbations also share a common function [26], with their coordinated response mediated by global regulators. In *E coli*, for example, the response to catabolic limitation (Fig. 11, red arrows) is mediated by cAMP-Crp [51], whereas the response to protein-synthesis inhibition is mediated by ppGpp [50]. Given the common architectural features in microbial metabolism

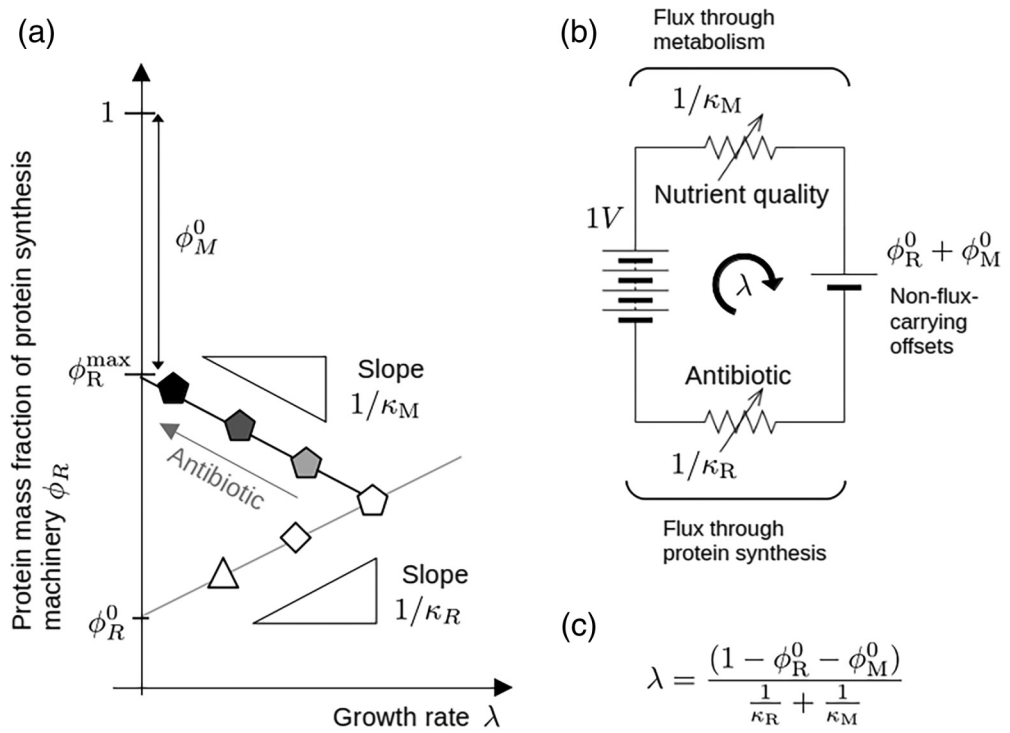

FIG. 10. (a) The open symbols are as in Fig. 8. Starting from a given growth medium, for example the medium supporting rapid growth (pentagon), increasing concentration of a ribosome-targeting antibiotic results in a negative linear correlation between the growth rate and the mass fraction of protein-synthesis proteins ϕ_R (increasing gray-scale). (b) In the simple circuit representation, the intercept in panel (a) provides an estimate of the offset associated with metabolic proteins, ϕ_M^0, and the slope provides the resistance $1/\kappa_M$ [29]. In that analogy, changes in nutrient quality act to modulate the metabolic resistor $1/\kappa_M$, whereas inhibition of protein synthesis modulates the resistor $1/\kappa_R$. (c) From the intersection of the two lines in panel (a), or from the circuit analogy in panel (b), the growth rate (current) can be expressed in terms of the four phenomenological parameters $\{\kappa_R, \kappa_M, \phi_R^0, \phi_M^0\}$.

(Fig. 5), the general topology of the metabolic network revealed by growth-inhibitory "probes" used on *E coli* is expected to be largely conserved among micro-organisms. Yet, given the tremendous variety of species-specific global regulatory logic [52,53], the growth-inhibitory probes used to query the network are likewise expected to exhibit tremendous species-specific variety.

Mathematical models of biological systems must balance the opposing demands of utility and simplicity. Gene deletion libraries [54], or libraries of individually inducible metabolic enzymes [55], can be used as "probes" at the level of single genes, and thereby provide a comprehensive mapping of the correlated expression of expressed proteins in a given growth environment [56]. The Thévenin-type coarse-graining is perhaps most relevant when perturbations identify a small set of phenomenological parameters that capture the system behavior in a comparatively simple model. Like the tension between hydrodynamic mean-field equations and molecular-dynamics simulation, or thermodynamics and statistical mechanics, the utility of a coarse-grained approach depends upon the experimental context and the details of the problem for which a mathematical model is the solution.

C. Ohmics

Flux balance analysis is a useful modeling framework that can be modified to accommodate a variety of additional constraints [57], including the constant protein concentration constraint [58]. However, the high-dimensional network fluxes it predicts can be difficult to analyze. The projection of these onto simple potential-resistor networks (an approach that Vincent Danos has called "Ohmics") provides a complementary mode of analysis. The resultant modeling framework provides several advantages over traditional flux-balance analysis.

(i) *Implicit direct global regulation*: Growth-inhibitory probes used to partition in the proteome identify large fractions of the proteome that are effectively regulated by a global effector. For example, proteins found in the *C* and *S* sectors in Fig. 11 are upregulated by cAMP-Crp, with *S* sector proteins exhibiting combinatorial control with whatever (currently unknown) effector upregulates the *A* sector proteins in response to anabolic limitation.

(ii) *Hierarchical coarse-graining*: Thévenin's theorem provides a theoretical justification for the decomposition of the proteome into increasingly-fine-grained sectors so that, for example, growth-inhibitory probes could be found to actively upregulate proteins responsible for fatty-acid or nucleotide synthesis.

(iii) *Indirect regulation and anticorrelated response*: The Ohmics circuit contains the constant-protein-concentration constraint implicitly as Kirchhoff's loop law [Eq. (20)]. The directed upregulation of one sector of the proteome can be used to infer the characterization of the

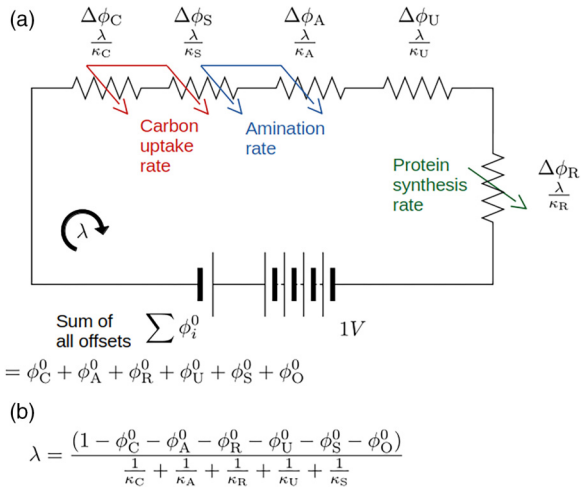

FIG. 11. (a) The concerted response of different proteins in response to different probes allows for a coarse-graining of the proteome. For example, in *E coli* modulating the carbon uptake rate (red) or the rate of amination (blue) further partitions the metabolic bow-tie in Fig. 5. In this way, Hui *et al.* [26] distinguish among proteins that are upregulated only in response to inhibition of carbon uptake (ϕ_C), those only upregulated to inhibition of the amination rate (ϕ_A), those that are upregulated along with both C and A proteins (ϕ_S), a growth-dependent fraction that is not upregulated by either probe (ϕ_U), and finally a sector exhibiting no growth rate dependence ($\phi_O = \phi_O^0$). The empirical growth dependence is summarized in the simple circuit, where the flux-carrying fraction of each protein sector is denoted by the potential drop across the resistors, $\Delta\phi_i$. (b) As with the two-sector coarse-graining shown in Fig. 10, with the nonribosomal proteins further divided into additional sectors, the growth rate λ is expressed in terms of 11 phenomenological parameters (the O sector carries no flux, and so there is no associated resistor $1/\kappa_O$).

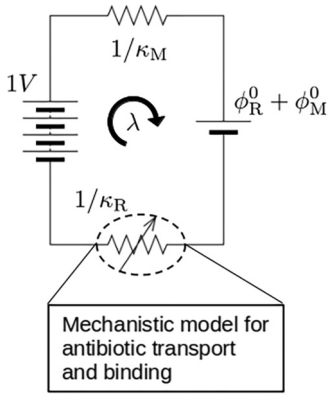

FIG. 12. A predictive model connecting antibiotic concentration with growth rate can be constructed using a mechanistic model for antibiotic transport and binding constrained to reproduce the empirical coupling between growth rate and the mass fraction of protein-synthesis proteins predicated on the physiological circuit.

remainder of the proteome, as was done in Fig. 10. Another consequence of the loop law is that if a non-flux-carrying heterologous protein is produced by *E coli*, effectively producing a synthetic offset, then the growth rate is predicted to decrease linearly with the mass fraction of the expressed protein [29], and this growth rate decrease is unavoidable.

Modification and extensions can be simply accommodated in this framework. For example, growth on two (or more) co-utilized carbon sources would introduce resistors arranged *in-parallel* within the $1/\kappa_C$ resistor shown in Fig. 11 [40,59]. In the next section, we consider in detail applications where the Ohmics model shown in Figs. 10(b) and 11 provides an essential physiological chassis.

VI. APPLICATIONS

The Ohmics framework provides a set of quantitative constraints that operate on mechanistic models. In this final section, two case studies are presented: growth-dependent susceptibility to ribosome-targeting antibiotics, and network constraints on evolutionary adaptation.

A. Interfacing physiological constraints with mechanistic models

In the previous section, ribosome-targeting antibiotics were used as a means to modulate the conductance κ_R through the ribosomal protein fraction in order to characterize the other coarse-grained elements in the circuit (see Fig. 9). But the relationship between the concentration of antibiotic and the growth rate is, itself, an important measure of antibiotic efficacy and of primary importance for the treatment of bacterial infection. To bridge the connection between applied antibiotic concentration and bacterial growth rate requires interfacing a mechanistic chemical-dynamics model for antibiotic transport and binding with the physiological "Ohmics" model (Fig. 12).

A simple model would contain, at minimum, the intracellular concentrations of the antibiotic (a), the unbound ribosome (r_u), and the bound ribosome (r_b). If the cells are growing with growth rate λ in the presence of an external antibiotic concentration, a_{ex}, then the three state variables are coupled via the governing differential equations,

$$\frac{da}{dt} = -\lambda a - k_{on} a r_u + k_{off} r_b + J(a, a_{ex}), \tag{23}$$

$$\frac{dr_u}{dt} = -\lambda r_u - k_{on} a r_u + k_{off} r_b + s(\lambda), \tag{24}$$

$$\frac{dr_b}{dt} = -\lambda r_b + k_{on} a r_u - k_{off} r_b, \tag{25}$$

where k_{on} and k_{off} characterize the binding and unbinding of the antibiotic, $J(a, a_{ex}) = P_{in} a_{ex} - P_{out} a$ is the transport of antibiotic in and out of the cell, and $s(\lambda)$ is the synthesis rate of new (unbound) ribosomes. This is a simple mechanistic model, and yet it is not solvable. First, the system is not closed: the growth rate, λ, is an unknown that is a desired output. Second, the synthesis rate $s(\lambda)$ is currently unspecified. Both of these difficulties are overcome by forcing the simple model to be consistent with the intrinsic coupling between the ribosomal content and the growth rate required by the "Ohmics" circuit [Fig. 10(a)].

In the absence of antibiotic, the growth rate depends linearly on the (unbound) ribosome concentration, and it is assumed that the same is true in the presence of antibiotics: $\lambda \propto \kappa_R r_u$ [Fig. 10(a), open symbols]. That provides a fourth equation determining λ and thereby closing the system. In the presence of antibiotics, at steady-state the *total* ribosome

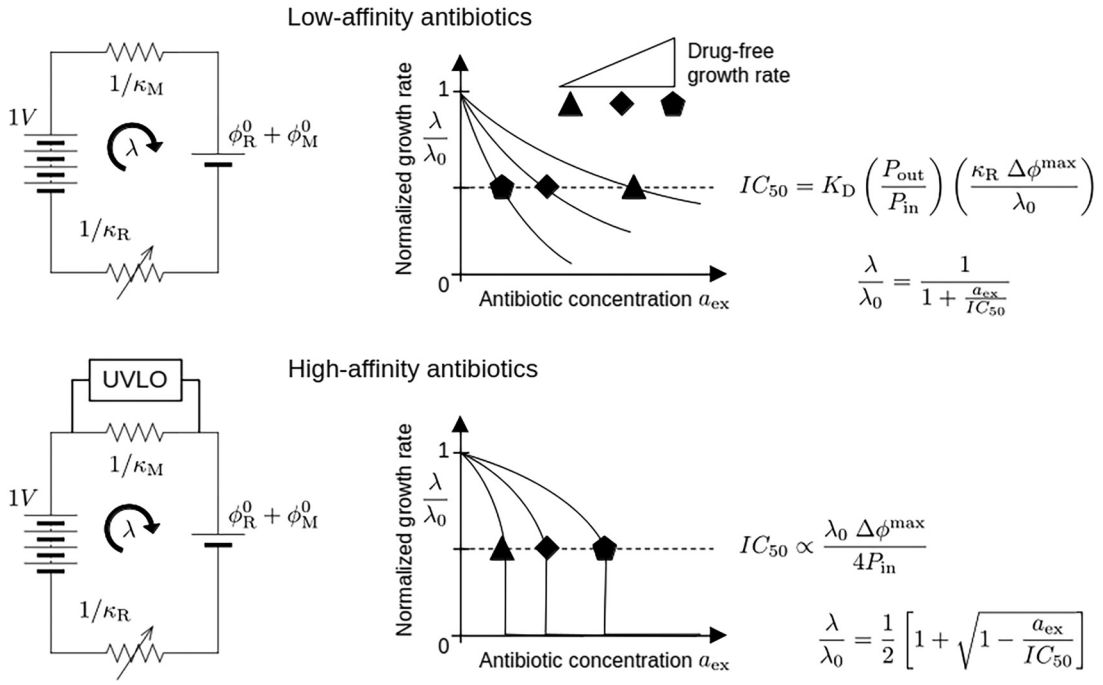

FIG. 13. The simple mechanistic model [Eq. (25)] produces qualitatively different behavior depending upon the binding affinity between the antibiotic and the ribosomal target [60]. For low-affinity binding antibiotics (e.g., chloramphenicol and tetracycline), both the model and experiments produce Langmuir-like inhibition curves, with half-inhibition concentration IC_{50} that is inversely related to the drug-free growth rate λ_0 (upper panels, symbols as in Fig. 8). Here, $\Delta\phi^{max} = 1 - \phi_R^0 - \phi_M^0$ denotes the maximum potential drop across the resistor $1/\kappa_R$. By contrast, for high-affinity binding antibiotics (e.g., kanamycin and streptomycin), the model and experiments produce sigmoidal inhibition curves, with half-inhibition concentration IC_{50} that is directly related to the drug-free growth rate. The constant of proportionality converts from mass-fraction on the right-hand side to concentration of the left. Furthermore, the abrupt drop in growth rate at the half-inhibition concentration behaves like an undervoltage lockout (UVLO) placed across the metabolic protein fraction.

concentration $r_u + r_b$ is again linearly dependent on the growth rate [Fig. 10(a), gray scale symbols]. The steady state of the second and third model equations [Eqs. (24) and (25)] defines the synthesis rate, $s(\lambda)$, as simply $\lambda \times$ the black line in Fig. 10(a) [60].

Solving the model equations [Eqs. (23)–(25)] at steady state, subject to the "Ohmics" constraints, reveals that ribosome-targeting antibiotics produce qualitatively different behavior based on their binding affinities. If the dissociation constant $K_D = k_{off}/k_{on}$ is large (as is the case with chloramphenicol and tetracycline), then the growth rate, λ, is a concave up function of the antibiotic concentration, and the half-inhibition concentration (Fig. 13, dashed) is negatively correlated with the drug-free growth rate. That is, low affinity ribosome-targeting antibiotics are more effective against fast-growing bacteria.

High-affinity antibiotics (such as the aminoglycosides kanamycin and streptomycin) exhibit qualitatively different behavior: the growth rate, λ, is a concave-down function of the concentrations of these antibiotics, and drops to zero growth at the half-inhibition concentration. In the "Ohmics" model, these high-affinity antibiotics effectively add an undervoltage lockout across the metabolic part of the circuit. Once the potential drop across the metabolic resistor, $1/\kappa_M$, drops below half its drug-free potential, the circuit breaks and the growth rate drops to zero. Furthermore, the half-inhibition concentration is positively correlated with the drug-free growth rate; high affinity ribosome-targeting antibiotics are more effective against slow-growing bacteria.

In Figs. 9 and 10, a low-affinity antibiotic was used as a probe to effectively increase the resistor $1/\kappa_R$. From the mechanistic model for antibiotic binding [Eqs. (23)–(25)], it would seem more appropriate to treat the antibiotic action as an increase in the offset, ϕ_R^0, corresponding to the nontranslating bound ribosomes, r_u. For the purposes of characterizing the nonribosomal circuit elements, all that matters is that the probe increases the potential drop across the protein-synthesis machinery (i.e., it results in a targeted increase in the protein mass fraction ϕ_R); for low affinity ribosome-targeting antibiotics, however, changes in the offset, ϕ_R^0, are equivalent to changes in the resistor, $1/\kappa_R$. This can be demonstrated by assuming equilibrium transport, so that the internal antibiotic concentration, a, is proportional to the external antibiotic concentration a_{ex}: $a = (P_{in}/P_{out})\, a_{ex}$, then making the substitution [46]

$$\kappa_R \mapsto \kappa_R^{max}\, \frac{a}{a + K_D}, \tag{26}$$

in the growth rate expression shown in Fig. 10(c). This produces the same growth rate, λ, as shown in the upper panel of Fig. 13. That is to say, for the low-affinity case, the effect of the ribosome-targeting antibiotic can be either thought of as a dynamic partitioning of the ribosomes into a subset that does not translate (r_b) and a subset translating at full-speed (r_u)

(this would be represented as a change in the offset ϕ_R^0), or as an averaged response where all ribosomes translate the same reduced rate given by Eq. (26) (this would be represented as a change in the resistance $1/\kappa_R$).

B. Network constraints on evolutionary adaptation

The "Ohmic" model quantitatively links the three primary constraints on the exponential growth of bacteria: flux balance, constant protein concentration, and enzyme-catalyzed reaction rates. On the long timescales of adaptive laboratory evolution, these same constraints persist if the majority of the proliferation time is spent in balanced growth.

There are several interesting tradeoffs that could arise when evolutionary selective pressure abuts intrinsic physiological constraints. Pinheiro *et al.* [61], for example, found that when *E coli* adapts to low concentrations of the high affinity ribosome-targeting antibiotic streptomyin, a common resistance pathway is a diminished function in nutrient uptake transporters that also uptake streptomycin. They model this as an effective *decrease* in the metabolic conductivity, κ_M, shown in Fig. 12, leading to a decreased drug-free growth rate. The tradeoff is that, for high affinity ribosome-targeting antibiotics, the antibiotic becomes more effective as the drug-free growth rate decreases (triangle in the lower panel of Fig. 12). Using a constrained metabolic model, the authors were able to quantitatively predict the coupling between the drug-free growth rate of the resistant mutants and the level of antibiotic resistance over a large range of antibiotic concentrations. Furthermore, they were able to predict the concentration of antibiotic exposure at which off-target transporter mutations became unfeasible, and mutations in the ribosome target began to dominate.

One would expect that similar "Ohmic" constraints would help direct adaptation trajectories under evolutionary selective pressure. One of the longest-running (and currently ongoing) adaptive laboratory evolution studies was started by Lenski in 1988 adapting *E coli* to growth in glucose and citrate as the sole carbon sources [62]. The six-component circuit analogy shown in Fig. 11 can be used to project the hundreds of genetic changes that accrued over the course of adaptation in this experiment onto the small set of phenomenological circuit parameters.

After 40 000 generations of adaptation in glucose, most of the circuit parameters remain unchanged except for a marked decrease in the offsets ϕ_O^0, ϕ_A^0, and ϕ_S^0. The decrease in ϕ_O^0 comes from a regulated decrease in the expression of an unnecessary porin, *OmpF* [63]. The decrease in ϕ_A^0 and ϕ_S^0 comes from enzymes in close network association with a deleted enzyme connecting glycolysis to the tricarboxylic acid (TCA) cycle, pyruvate kinase *PykF* [39].

The enzyme *PykF* is the target of a flux-sensing mechanism [64,65] that acts as a speedometer coordinating the flux through upper glycolysis with the flux through the TCA cycle. The "Ohmic" analysis of the Lenski strains led Mori *et al.* [39] to a simple mechanistic model that extends the analysis in Sec. III from irreversible kinetics to include allosteric regulation and reversibility. Their claim is that deletion of the flux-sensing mechanism mediated by *PykF* leads to an increase in enzyme efficiency via substrate saturation, and they predict that loss of flux-sensing mechanisms could be a generic response to evolutionary adaptation.

VII. CONCLUSIONS

Mathematical models of biological systems can be overwhelmingly complex. Bacterial growth physiology, however, is characterized by simple empirical constraints linking gene expression and growth rate that promise a similarly simple predictive framework governing suitably chosen state variables [1,33].

In balanced growth, the empirical constraint of near-invariant protein concentration, along with the ubiquity of enzyme-catalyzed reaction kinetics, provides a mathematical framework for linking protein mass fraction and reaction flux to growth rate under a range of growth conditions. This "Ohmics" approach is a one-to-one mapping of electrical circuit analysis applied to a collection of resistors and batteries. The framework, beyond computational efficiency, inherits the operating constraints of electric circuits (including Thévenin equivalence) that provide a mechanistic justification for coarse-graining complex biochemical reaction networks into simple circuit analogies.

The biochemical origin of the resulting phenomenological circuit parameters has only recently been clarified in the case of irreversible enzyme kinetics [24], and more generally applied in the context of reversible kinetics subject to post-transcriptional regulation [39]. By way of illustration, we discuss several case studies where simple mechanistic models yield unexpected, but experimentally verifiable, conclusions when tethered to an Ohmics chassis [39,60,61].

Constraints-based metabolic network analysis shares the limitations of any phenomenological theory insofar as they capture coarse-grained empirical behavior but are agnostic to the mechanistic origins of that behavior. As with the analysis of electrical phenomena [66], it can be challenging to rationalize how molecular interactions give rise to simple empirical relations [50]. Metabolic network analysis is further limited by the heterogeneous implementation of network connectivity. For an electrical circuit, the wires and resistors are homogeneous, static building blocks, and modulating the current through any particular wire is straightforward. In contrast, the connecting elements among the nodes of a metabolic network are a mixture of chemically distinct substrate and effector molecules. Identifying modes of growth inhibition [e.g., the "probes" in Fig. 11(a)] that lay bare the coarse-grained structure of the network requires educated guesswork, and there is no reason to suppose that the same probes that have been successful in the analysis of *E coli* will have the same success in other organisms.

For a physicist, bacterial physiology presents an interesting historical inversion. Whereas in physics the macroscopic thermodynamic investigations of the 1800s gave way to the microscopic statistical mechanics of the early 1900s, in microbiology we have something like the reverse. The past 50 years have seen a proliferation of large-Ohmics data sets under a wide variety of growth conditions for multifarious organisms. Like Kepler with Brahe's notebooks, this wealth of data presents the opportunity for "synthetic" biology in the alchemical sense: synthesizing disparate details into an intelligible whole.

[1] J. Monod, The growth of bacterial cultures, Annu. Rev. Microbiol. **3**, 371 (1949).

[2] A. Campbell, Synchronization of cell division, Bacteriol. Rev. **21**, 263 (1957).

[3] M. Schaechter, From growth physiology to systems biology, Int. Microbiol. **9**, 157 (2006).

[4] H. Bremer and P. P. Dennis, Modulation of chemical composition and other parameters of the cell by growth rate, in *Escherichia coli and Salmonella: Cellular and Molecular Biology*, edited by F. C. Neidhardt and R. Curtiss (ASM, Washington, DC, 1996), pp. 1553–1569.

[5] F. C. Neidhardt, P. L. Bloch, and D. F. Smith, Culture medium for enterobacteria, J. Bacteriol. **119**, 736 (1974).

[6] K. Stevenson, A. F. McVey, I. B. N. Clark, P. S. Swain, and T. Pilizota, General calibration of microbial growth in microplate readers, Sci. Rep. **6**, 38828 (2016).

[7] E. T. Papoutsakis, Equations and calculations for fermentations of butyric acid bacteria, Biotechnol. Bioeng. **26**, 174 (1984).

[8] A. Varma and B. O. Palsson, Metabolic flux balancing: Basic concepts, scientific and practical use, Nat. Biotechnol. **12**, 994 (1994).

[9] L. Heirendt, S. Arreckx, T. Pfau, S. N. Mendoza, A. Richelle, A. Heinken, H. S. Haraldsdóttir, J. Wachowiak, S. M. Keating, V. Vlasov, S. Magnusdóttir, C. Y. Ng, G. Preciat, A. Žagare, S. H. Chan, M. K. Aurich, C. M. Clancy, J. Modamio, J. T. Sauls, A. Noronha *et al.*, Creation and analysis of biochemical constraint-based models using the COBRA Toolbox v.3.0, Nat. Protoc. **14**, 639 (2019).

[10] A. Ebrahim, J. A. Lerman, B. O. Palsson, and D. R. Hyduke, COBRApy: Constraints-based reconstruction and analysis for python, BMC Syst. Biol. **7**, 74 (2013).

[11] L. Heirendt, I. Thiele, and R. M. Fleming, DistributedFBA.jl: High-level, high-performance flux balance analysis in Julia, Bioinformatics **33**, 1421 (2017).

[12] Z. A. King, J. Lu, A. Dräger, P. Miller, S. Federowicz, J. A. Lerman, A. Ebrahim, B. O. Palsson, and N. E. Lewis, BiGG Models: A platform for integrating, standardizing and sharing genome-scale models, Nucl. Acids Res. **44**, D515 (2016).

[13] C. Lieven, M. E. Beber, B. G. Olivier, F. T. Bergmann, M. Ataman, P. Babaei, J. A. Bartell, L. M. Blank, S. Chauhan, K. Correia, C. Diener, A. Dräger, B. E. Ebert, J. N. Edirisinghe, J. P. Faria, A. M. Feist, G. Fengos, R. M. Fleming, B. García-Jiménez, V. Hatzimanikatis *et al.*, MEMOTE for standardized genome-scale metabolic model testing, Nat. Biotechnol. **38**, 272 (2020).

[14] J. D. Orth, I. Thiele, and B. O. Palsson, What is flux balance analysis?, Nat. Biotechnol. **28**, 245 (2010).

[15] R. Mahadevan, J. S. Edwards, and F. J. Doyle III, Dynamic flux balance analysis of diauxic growth in *Escherichia coli*, Biophys. J. **83**, 1331 (2002).

[16] S. Gudmundsson and I. Thiele, Computationally efficient flux variability analysis, BMC Bioinf. **11**, 489 (2010).

[17] N. E. Lewis, K. K. Hixson, T. M. Conrad, J. A. Lerman, P. Charusanti, A. D. Polpitiya, J. N. Adkins, G. Schramm, S. O. Purvine, D. Lopez-Ferrer, K. K. Weitz, R. Eils, R. König, R. D. Smith, and B. Palsson, Ohmic data from evolved *E. coli* are consistent with computed optimal growth from genome-scale models, Mol. Syst. Biol. **6**, 390 (2010).

[18] J. Zanghellini, D. E. Ruckerbauer, M. Hanscho, and C. Jungreuthmayer, Elementary flux modes in a nutshell: Properties, calculation and applications, Biotechnol. J. **8**, 1009 (2013).

[19] F. M. Menger, An alternative view of enzyme catalysis, Pure Appl. Chem. **77**, 1873 (2005).

[20] K. A. Johnson and R. S. Goody, The original Michaelis constant: Translation of the 1913 Michaelis–Menten paper, Biochemistry **50**, 8264 (2011).

[21] G. E. Briggs and J. B. S. Haldane, A note on the kinetics of enzyme action, Biochem. J. **19**, 338 (1925).

[22] J. Eilertsen, S. Schnell, and S. Walcher, The unreasonable effectiveness of the total quasi-steady state approximation, and its limitations, J. Theor. Biol. **583**, 111770 (2024).

[23] A. Cornish-Bowden, *Fundamentals of Enzyme Kinetics*, 4th ed. (Wiley-Blackwell, Weinheim, Germany, 2012).

[24] H. Dourado, M. Mori, T. Hwa, and M. J. Lercher, On the optimality of the enzyme–substrate relationship in bacteria, PLoS Biol. **19**, e3001416 (2021).

[25] J. Monod, J. Wyman, and J. P. Changeux, On the nature of allosteric transitions: A plausible model, J. Mol. Biol. **12**, 88 (1965).

[26] S. Hui, J. M. Silverman, S. S. Chen, D. W. Erickson, M. Basan, J. Wang, T. Hwa, and J. R. Williamson, Quantitative proteomic analysis reveals a simple strategy of global resource allocation in bacteria, Mol. Syst. Biol. **11**, 784 (2015).

[27] F. C. Neidhardt and B. Magasanik, Studies on the role of ribonucleic acid in the growth of bacteria, Biochim. Biophys. Acta **42**, 99 (1960).

[28] A. Pavlou, E. Cinquemani, C. Pinel, N. Giordano, V. M.-G. Mathilde, I. Mihalcescu, J. Geiselmann, and H. de Jong, Single-cell data reveal heterogeneity of investment in ribosomes across a bacterial population, Nat. Commun. **16**, 285 (2025).

[29] M. Scott, C. W. Gunderson, E. M. Mateescu, Z. Zhang, and T. Hwa, Interdependence of cell growth and gene expression: Origins and consequences, Science **330**, 1099 (2010).

[30] M. Mori, Z. Zhang, A. Banaei-Esfahani, J.-B. Lalanne, H. Okano, B. C. Collins, A. Schmidt, O. T. Schubert, D.-S. Lee, G.-W. Li, R. Aebersold, T. Hwa, and C. Ludwig, From coarse to fine: the absolute *Escherichia coli* proteome under diverse growth conditions, Mol. Syst. Biol. **17**, e9536 (2021).

[31] S. Klumpp, M. Scott, S. Pedersen, and T. Hwa, Molecular crowding limits translation and cell growth, Proc. Natl. Acad. Sci. USA **110**, 16754 (2013).

[32] S. Cooper, *Bacterial Growth and Division: Biochemistry and Regulation of the Division Cycle of Prokaryotes and Eukaryotes*, 1st ed. (Academic Press, New York, NY, 1991).

[33] M. Schaechter, O. Maaløe, and N. O. Kjeldgaard, Dependency on medium and temperature of cell size and chemical composition during balanced growth of Salmonella typhimurium, J. Gen. Microbiol. **19**, 592 (1958).

[34] S. Taheri-Araghi, S. Bradde, N. Hill, P. A. Levin, J. Paulsson, M. Vergassola, and S. Jun, Cell size control and homeostasis in bacteria, Curr. Biol. **25**, 385 (2015).

[35] E. R. Oldewurtel, Y. Kitahara, and S. van Teeffelen, Robust surface-to-mass coupling and turgor-dependent cell width determine bacterial dry-mass density, Proc. Natl. Acad. Sci. USA **118**, e2021416118 (2021).

[36] R. Balakrishnan, M. Mori, I. Segota, Z. Zhang, R. Aebersold, C. Ludwig, and T. Hwa, Principles of gene regulation quantitatively connect DNA to RNA and proteins in bacteria, Science **378**, eabk2066 (2022).

[37] J. van den Berg, A. J. Boersma, and B. Poolman, Microorganisms maintain crowding homeostasis, Nat. Rev. Microbiol. **15**, 309 (2017).

[38] M. Scott and T. Hwa, Shaping bacterial gene expression by physiological and proteome allocation constraints, Nat. Rev. Microbiol. **21**, 327 (2023).

[39] M. Mori, V. Patsalo, C. Euler, J. R. Williamson, and M. Scott, Proteome partitioning constraints in long-term laboratory evolution, Nat. Commun. **15**, 4087 (2024).

[40] S. Jun, F. Si, R. Pugatch, and M. Scott, Fundamental principles in bacterial physiology - history, recent progress, and the future (with focus on cell size control), Rep. Prog. Phys. **81**, 056601 (2018).

[41] L. H. Hartwell, J. J. Hopfield, S. Leibler, and A. W. Murray, From molecular to modular cell biology, Nature (London) **402**, C47 (1999).

[42] M. Csete and J. Doyle, Bow ties, metabolism and disease, Trends Biotechnol. **22**, 446 (2004).

[43] R. Braakman and E. Smith, The compositional and evolutionary logic of metabolism, Phys. Biol. **10**, 011001 (2013).

[44] F. C. Neidhardt, J. L. Ingraham, and M. Schaechter, *Physiology of the Bacterial Cell: A Molecular Approach*, 1st ed. (Sinaur, Sunderland, MA, 1990).

[45] G. Caetano-Anollés, L. S. Yafremava, H. Gee, D. Caetano-Anollés, H. S. Kim, and J. E. Mittenthal, The origin and evolution of modern metabolism, Int. J. Biochem. Cell Biol. **41**, 285 (2009).

[46] M. Scott, S. Klumpp, E. M. Mateescu, and T. Hwa, Emergence of robust growth laws from optimal regulation of ribosome synthesis, Mol. Syst. Biol. **10**, 747 (2014).

[47] C. Hinshelwood, Autosynthesis, J. Chem. Soc. **0**, 1947 (1953).

[48] A. L. Koch, Why can't a cell grow infinitely fast?, Can. J. Microbiol. **34**, 421 (1988).

[49] B. J. Paul, W. Ross, and R. L. Gourse, rRNA transcription in *Escherichia coli*, Annu. Rev. Genet. **38**, 749 (2004).

[50] C. Wu, R. Balakrishnan, N. Braniff, M. Mori, G. Manzanarez, Z. Zhang, and T. Hwa, Cellular perception of growth rate and the mechanistic origin of bacterial growth law, Proc. Natl. Acad. Sci. USA **119**, e2201585119 (2022).

[51] C. You, H. Okano, S. Hui, Z. Zhang, M. Kim, C. W. Gunderson, Y. P. Wang, P. Lenz, D. Yan, and T. Hwa, Coordination of bacterial proteome with metabolism by cyclic AMP signalling, Nature (London) **500**, 301 (2013).

[52] M. Nomura, Regulation of ribosome biosynthesis in *Escherichia coli* and Saccharomyces cerevisiae: Diversity and common principles, J. Bacteriol. **181**, 6857 (1999).

[53] B. Görke and J. Stülke, Carbon catabolite repression in bacteria: many ways to make the most out of nutrients, Nat. Rev. Microbiol. **6**, 613 (2008).

[54] T. Baba, T. Ara, M. Hasegawa, Y. Takai, Y. Okumura, K. A. D. M. Baba, M. Tomita, B. L. Wanner, and H. Mori, Construction of *Escherichia coli* k-12 in-frame, single-gene knockout mutants: The Keio collection, Mol. Syst. Biol. **2**, 2006.0008 (2006).

[55] M. Kitagawa, T. Ara, M. Arifuzzaman, T. Ioka-Nakamichi, E. Inamoto, H. Toyonaga, and H. Mori, Complete set of ORF clones of *Escherichia coli*: ASKA library, DNA Res. **12**, 291 (2005).

[56] J. P. Côté, S. French, S. S.Gehrke, C. R. MacNair, C. S. Mangat, A. Bharat, and E. D. Brown, The genome-wide interaction network of nutrient stress genes in *Escherichia coli*, mBio **7**, e01714-16 (2016).

[57] J. Schellenberger, R. Que, R. M. T. Fleming, I. Thiele, J. D. Orth, A. M. Feist, D. C. Zielinski, A. Bordbar, N. E. Lewis, S. Rahmanian, J. Kang, D. R. Hyduke, and B. O. Palsson, Quantitative prediction of cellular metabolism with constraint-based models: The COBRA Toolbox v2.0, Nat. Protocols **6**, 1290 (2011).

[58] M. Mori, T. Hwa, O. C. Martin, A. D. Martino, and E. Marinari, Constrained allocation flux balance analysis, PLoS Comput. Biol. **12**, e1004913 (2016).

[59] R. Hermsen, H. Okano, C. You, N. Werner, and T. Hwa, A growth-rate composition formula for the growth of *E. coli* on co-utilized carbon substrates, Mol. Syst. Biol. **11**, 801 (2015).

[60] P. Greulich, M. Scott, M. R. Evans, and R. J. Allen, Growth-dependent bacterial susceptibility to ribosome-targeting antibiotics, Mol. Syst. Biol. **11**, 796 (2015).

[61] F. Pinheiro, O. Warsi, D. I. Andersson, and M. Lässig, Metabolic fitness landscapes predict the evolution of antibiotic resistance, Nat. Ecol. Evol. **5**, 677 (2021).

[62] J. E. Barrick, D. S. Yu, S. H. Yoon, H. Jeong, T. K. Oh, D. Schneider, R. E. Lenski, and J. F. Kim, Genome evolution and adaptation in a long-term experiment with *Escherichia coli*, Nature (London) **461**, 1243 (2009).

[63] E. Crozat, T. Hindré, L. Kühn, J. Garin, R. E. Lenski, and D. Schneider, Altered regulation of the ompf porin by fis in *Escherichia coli* during an evolution experiment and between b and k-12 strains, J. Bacteriol. **193**, 429 (2011).

[64] K. Kochanowski, B. Volkmer, L. Gerosa, B. R. H. van Rijsewijk, A. Schmidt, and M. Heinemann, Functioning of a metabolic flux sensor in *Escherichia coli*, Proc. Natl. Acad. Sci. USA **110**, 1130 (2013).

[65] C. Euler and R. Mahadevan, On the design principles of metabolic flux sensing, Biophys. J. **121**, 237 (2022).

[66] J. Jang and N. Masmoudi, Derivation of Ohm's law from the kinetic equations, SIAM J. Math. Anal. **44**, 3649 (2012).